Effects of sterilization on nanogel-based universal coatings

Ghosh, Devlina; Peterson, Brandon W.; de Waal, Cees; de Vries, Joop; Kaper, Hans; Zu, Guangyue; Witjes, Max; van Rijn, Patrick

Published in:
Materials and Design

DOI:
10.1016/j.matdes.2024.112689

Publication date:
2024

Materials & Design 238 (2024) 112689

Contents lists available at ScienceDirect

Materials & Design

journal homepage: www.elsevier.com/locate/matdes

Effects of sterilization on nanogel-based universal coatings: An essential step for clinical translation

Devlina Ghosh [a], Brandon W. Peterson [a], Cees de Waal [c], Joop de Vries [a], Hans Kaper [a], Guangyue Zu [a], Max Witjes [b], Patrick van Rijn [a,*]

[a] University of Groningen, University Medical Center Groningen, Department of Biomedical Engineering-FB40, Antonius Deusinglaan 1, 9713 AV Groningen, the Netherlands
[b] University of Groningen, University Medical Center Groningen, Department of Oral and Maxillofacial Surgery, Hanzeplein 1 BB70, 9713 GX Groningen, the Netherlands
[c] SteriNoord, Jeverweg 3e, 9723 JE Groningen, the Netherlands

ARTICLE INFO

Keywords:
Nanogel
Sterilization
Coating
Antifouling
Bacterial adhesion

ABSTRACT

Implant associated infections are a serious threat to the well-being of patients, which can be mitigated by taking effective disinfection/sterilization (D/S) methods into account. Nanogels (nGel) are stimuli sensitive polymeric hydrogel particles, which have provided numerous innovative applications in the biomedical field to enhance antifouling, antibacterial properties, or drug delivery, or they can be employed as imaging modalities or can be applied as a coating on biomaterials (implants). Prior to translating their application towards clinical use, nGel-based coated implant materials must undergo an intermediary, pre-requisite process of cleaning, disinfection, and sterilization, in sequence. The interplay among the three crucial pillars- the implant material, the nGel coating (with specific function), and the applied D/S processes influence the fate (success or failure) of medical implant in the host body. In this study, we investigated a previously developed NIPAM-*co*-APMA core shell nGel coating on various clinically-relevant polymeric and inorganic implant materials and tested them on a diverse range of D/S techniques to assess the retention of the coating quality and antifouling function. The stability and integrity of the nGel coating was analyzed by performing Atomic Force Microscopy and the retention of the antifouling function of the nGel-coating after sterilization was studied by Colony forming units against *S. aureus* RN4220. Among all the materials that were coated, polymeric materials- polypropylene and polyetheretherketone exhibited exceptional coating stability, post-sterilization while also demonstrating a considerable reduction in bacterial attachment with respect to their 'uncoated, sterilized' and 'coated, non-sterilized' controls. Although often overlooked, sterilization is an indispensable part of clinical translation, therefore research in this domain is of utmost importance when considering clinical translatability.

1. Introduction

Nosocomial or Health-care Associated Infections (HAI) are infections that are transmitted to patients during their visit or stay in a healthcare facility and that were not present prior to their visit. HAI has an occurrence of 7 % in developed countries and as high as 10 % in developing countries [1–3]. The most prevalent form of HAIs is seen in blood, respiratory or urinary tract infections. Surgical site infections often occur on medical devices and implants which can be introduced by pre-existing infections/commensal bacteria, patients, hospital staff, unhygienic environment, and other visitors [4,5]. HAIs are spread by nosocomial pathogens such as bacteria (*Pseudomonas aeruginosa*, *Escherichia coli*, *Staphylococcus aureus)*, fungal parasites *(Candida albicans)*, or viruses (influenza) [3,6]. Therefore, sterilization is an essential pre-requisite for undergoing any invasive and non-invasive clinical procedures, diagnosis, or surgery, including medical devices that contain an antifouling coating with antibacterial properties.

Disinfection and sterilization should always be preceded by cleaning, and these processes exhibit well-defined functions at the clinical level [7]. Cleaning is the first crucial step that involves removal of bioburden, dust, or dirt from the biomaterial/ medical device [8]. This is followed by disinfection, which is the removal of any body fluids, debris or visible

* Corresponding author.
E-mail address: p.van.rijn@umcg.nl (P. van Rijn).

https://doi.org/10.1016/j.matdes.2024.112689
Received 11 August 2023; Received in revised form 15 December 2023; Accepted 19 January 2024
Available online 26 January 2024

contaminants, and consequently the final crucial step is sterilization, which facilitates the complete eradication and inhibition of reproduction and growth of any microorganisms such as, bacteria, fungi, or spores using several physical and chemical processes [9,10]. Some of the clinically-approved disinfection/sterilization (D/S) techniques include low-level disinfection at primary level with 70 % ethanol [11], heat sterilization by autoclaving at 121 °C or 134 °C [12], chemical treatments by hydrogen peroxide gas plasma (HPGP) [13], and non-ionizing irradiation by Ultraviolet-C (UV-C) at 254 nm, which is close to the desirable wavelength (262 nm) required to achieve germicidal activity [14–16]. Therefore, only after undergoing these processes, the material is free of any pathogenic or non-pathogenic entity and can be defined as 'sterile'[17]. The end goal of sterilization is to reduce the level of microbial contaminants to a permissible amount, without hampering the quality/integrity and functionality of the material [18]. Owing to the importance of sterilization, Scheme 1 illustrates the sequential steps that are involved in the development of nanogel (nGel)-coated implant materials through clinically-relevant D/S techniques, without which clinical implementation will not be possible. Post-sterilization function, the stability of the coating, and the retention of its function (hereafter, antifouling) were studied. If the coating and its function remain intact, it can be considered for further clinical applications, otherwise the coated materials must be re-designed to withstand clinical D/S approaches.

Here, we have implemented *N*-isopropylacrylamide–*co*-*N*-(3-aminopropyl)methacrylamide dihydrochloride (NIPAM-*co*-APMA) nGel-based coatings on the implant surfaces via electrostatic adherence. nGels are crosslinked, nano-sized colloidal particles of which the physicochemical properties [19–21] can be easily tuned by stimuli-responsiveness to temperature [22], pH [23], ionic strength [24], light [25], or co-solvents [26]. Coatings act as an interface between the implant material and the external environment [27,28]. Therefore, coatings help in enhancing the material properties and have also proven to be very promising for introducing different functionalities such as, antifouling and antibacterial moieties [21,29,30], drugs [31–33], imaging modalities [34], or for immunomodulation of host response [35]. These hydrophilic polymer hydrogel particles, when applied as a coating, act as a hydration layer, thereby creating an antifouling coating that prevents the adsorption of different biomolecules and microorganisms [30,31,36]. Previously, our group has demonstrated the tunability of the antifouling function of the poly-N-isopropylmethacrylamide (pNIPMAM) nGel coating based on the size and stiffness of the nGel particles, as well as the thickness of the coating that resulted up to 98 % reduction of *S.aureus* ATCC 12600 when P(NIPMAM) nGel coatings were applied on glass [37]. The applicability of the coating was drastically enhanced upon development of a universal electrostatic method to apply the same coating via the same procedure for many other clinically and industrially-relevant materials [28,38]. In order to assess potential clinical translation, here the aim of our research is to investigate the NIPAM-*co*-APMA nGel coating integrity, stability, and antifouling function after using a range of D/S processes, both in-house (IH; 70 % ethanol; autoclave at 121 °C; UV-C radiation) and outsourced commercially-relevant [CR; disinfection at low temperature (LT; ~80 °C); disinfection LT + sterilization by HPGP at 90 °C; disinfection at high temperature (HT; ~115 °C); and disinfection HT + sterilization by autoclave at 134 °C] at SteriNoord BV, Groningen, the Netherlands on the nGel coated implant materials. The integrity of the coatings was assessed by Atomic Force microscopy (AFM) while the effectiveness of the antifouling function of the sterilized nGel-coated surfaces of the implant materials were analysed by enumeration on agar plates for Colony Forming Units (CFU) against *S.aureus* RN4220. The findings reaffirmed the necessity of sterilization and provided valuable insights on the optimal sterilization techniques that can be used for the nGel-coated implant surfaces based on electrostatic interactions. There is no single D/S technique that is compatible for all classes of medical implants (bioglass/ceramic, metallic, fluorinated, polymers and elastomers) [28], therefore, we aimed to identify the optimal sterilization technique suited for different nGel-coated implant materials.

2. Materials and methods

2.1. Materials

Primary monomer, N-Isopropylacrylamide (>98 %, NIPAM) was acquired from Tokyo Chemical Industry (TCI), Belgium, the co-monomer N-(3-aminopropyl)methacrylamide dihydrochloride (>98 %,

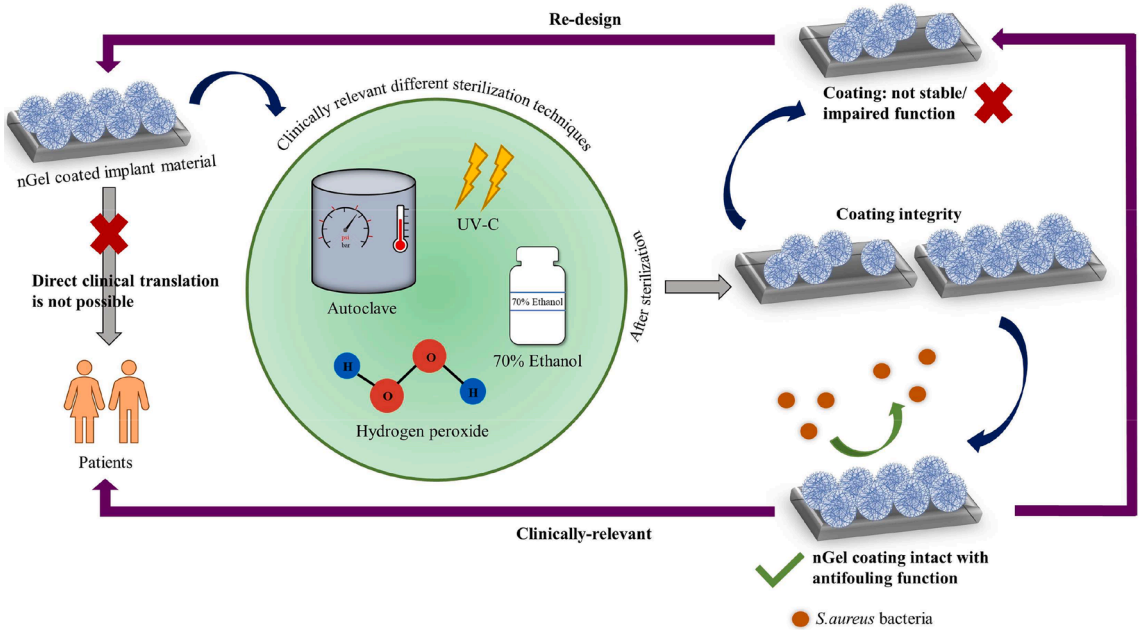

Scheme 1. Schematic illustration to demonstrate D/S as the necessary step (Autoclave, Hydrogen peroxide, 70% ethanol, irradiation by ultraviolet-C) between the development of the nGel-coated implant surfaces (bench) and their application in the clinic. Post-sterilization, there are two important factors to be considered, **(i)** the coating integrity on the surface of the material and **(ii)** the retention of function, in this case antifouling. Upon failing either of these aspects, the coated materials must be redesigned to enable their clinical translation/application.

APMA) was procured from Polysciences, Inc., Germany. The cross-linker N,N′-methylenebis(acrylamide) (99 %, BIS); surfactant hexadecyltrimethylammonium bromide (>99 %, CTAB); and initiator 2,2′-azobis (2-methylpropionamidine) dihydrochloride (97 %, V50) were obtained from Sigma-Aldrich, The Netherlands. NIPAM was purified by recrystallized from hexane, and all the other chemicals were used, without any further purification. For all the experiments, ultra-pure water was used (18.2 MΩ, arium 611 DI water purification system; Sartorius AG, Germany). A range of different and unique clinically available implant materials were used: glass, polytetrafluoroethylene (PTFE; Teflon), polymethylmethacrylate (PMMA), silicone rubber (Si-rubber), Polypropylene (PP), Polyetheretherketon (PEEK), titanium, Stainless steel (SS). Glass was obtained from Thermo Scientific Menzel-Gläser (Gerhard Menzel B.V. & Co. KG, Braunschweig, Germany), while the other materials were procured from the Research Instrument Laboratory at the University Medical Center Groningen (UMCG). Detailed information regarding the materials is indicated in **Table S1**.

2.2. nGel synthesis and particle characterization

p(NIPAM-*co*-AMPA) core shell nGel was synthesized by precipitation polymerization reaction, according to the approach reported before [28]. Briefly, the reaction was carried out in a 250 ml three-necked round bottom flask equipped with an inlet/outlet for nitrogen, thermometer and a reflux condensor. Primary monomer, NIPAM (1505 mg); crosslinker, BIS (108 mg); and surfactant, CTAB (4 mg) were dissolved in 95 ml of ultrapure water, followed by degassing the main solution for 1 hr in N_2 and heating to 70 °C. In the following step, degassed initiator, APMA V50 (54 mg), dissolved in 5 ml of ultrapure water was added to the main solution. The initiation of the polymerization was indicated by turning of the clear solution to a milky-white suspension, which resulted in the formation of the core of the nGel. In the final step, the shell part of the nGel was synthesized by dissolving NIPAM (673 mg); co-monomer, APMA (125 mg); BIS (54 mg), and CTAB (2 mg) to 50 ml ultrapure water and degassed under N_2 for 1 hr. The shell solution was injected to the polymerized turbid suspension in a dropwise manner, and the synthesis was carried out in an inert environment for 6 hr at 70 °C, followed by overnight stirring under room temperature. For purification, the nGel suspension was centrifuged at 16,000 rpm (38,300 g) thrice, for 1 h each and dialyzed (MWCO = 3.5 Kda) against water for 3 days, while changing the water twice per day. Finally, the suspension was lyophilized for 3 days and the positively-charged NIPAM-*co*-APMA nGel particles were stored for further use.

Particle characterization was performed using a ZetaSizer Nano-ZS equipment (Malvern Instruments, Worcestershire, U.K.) with a wavelength of laser beam at 633 nm to determine the temperature-dependent hydrodynamic diameter (D_h) by ranging the temperature from 24 °C to 60 °C with an interval of 2 °C by Dynamic Light Scattering (DLS) and zeta potential at 24 °C. In order to avoid multiple scattering during the measurement, the suspension was diluted to 0.5 mg/ml in ultrapure water. The measurements for D_h were carried out in disposable cuvettes and the instruments operated at 173°, while the zeta potential was measured in disposable folded capillary cuvette and at a fixed angle of 17°. The final results from the DLS and zeta potential were the average of 3 consecutive readings performed on the same nGel suspension. The morphology of the nGel particles in their dry state was acquired by Transmission Electron Microscopy (TEM). Here, the particles were drop casted on a carbon film which is coated with a copper grid were negatively stained by uranyl acetate, and were investigated by Philips CM_{120} microscope fitted to a 4 k CCD camera with an acceleration voltage of 120 kV.

2.3. Formation of coating

The coating was applied following the previously mentioned procedure [37]. Briefly, the nGel particles were dissolved in ultrapure water at a concentration of 5 mg/ml (0.5 wt%). The suspension was sonicated (Transsonic TP690, Salm en Kipp B.V., the Netherlands) for 10 min to break any aggregates in the suspension. Meanwhile, the surface of the material was cleaned by 70 % ethanol then by ultrapure water and dried with pressurized air. In the following step, the surface was pre-treated by plasma oxidation for 10 min (100 mTorr and 0.2 mbar, on Plasma Active Flecto 10 USB). Subsequently, the surface of the materials was coated using a spraying device by tilting at an angle of 45°. The spraying device dispersed 140 μL per spray and it was carried on until the surface was coated completely. The coated surfaces were dried by keeping them at room temperature for 2 h, followed by drying in the oven at 50 °C, overnight. To achieve a homogenous, monolayer of the nGel coating on the material surface, they were immersed in ultrapure water for 6 h while changing the water three times.

2.4. Analysis of coating thickness by Ellipsometer

The thickness of the nGel coating was measured on silicon wafer substrate by Ellipsometer (EL X–02C, DRE, Ratzeburg, Germany). The independent measurements were taken with a laser of 632 nm and at an incidence angle of 65°. The thickness of the layer was computed from the amplitude ratio (Ψ) and the relative phase shift data (Δ) using an in-house built MATLAB script [39].

2.5. Disinfection/ sterilization (D/S) techniques

A diverse range of IH and CR (SteriNoord BV, Groningen, The Netherlands) D/S techniques were employed on the nGel-coated materials. For the IH D/S processes, **(i)** implant materials were autoclaved at 121 °C, 209 kPa (or, 2.09 bar) for 20 min; **(ii)** disinfected thrice by submerging in 70 % ethanol (low-level disinfectant), followed by ultrapure water for 15 min each (alternatingly) and **(iii)** irradiated by UV-C at 254 nm, ~0.3 mW/cm^2 (LAC Labs UG, 53,639 Königswinter, Germany). The CR techniques included **(i)** disinfection at low temperature (~80 °C) and succeeded by sterilization by HPGP at 90 °C, 66.66 Pa (or, 0.66 mbar); and **(ii)** disinfection at HT (~115 °C), subsequently sterilization by autoclave at 134 °C, 313 kPa (or, 3.13 bar) for 5 min using SteriNoord facilities where clinical D/S processes are done for most hospitals in northern Netherlands.

2.6. Analysis of coating stability by AFM

The stability of the coating after the sterilization process was indicated by the presence of the nGel particles on the material surface, and it was determined by the AFM measurements in the dry state. The coating stability was analysed on four categories of samples **(i)** non-coated and non-sterilized; **(ii)** non-coated and sterilized; **(iii)** coated and non-sterilized materials and **(iv)** coated and sterilized, using the Bruker model DNP-10 tip (consisting of non-conductive silicon nitride, spring constant of 0.24 N/m) in contact mode. The scanning area was maintained at 10x10μm^2, while ensuring that the measurements were taken around the center of the coated material surfaces to avoid any deflections in the captured images caused by removal of the coating due to human error. Finally, the raw data were assessed by NanoScope Analysis (version 1.80) software.

2.7. Analysis of change in wettability by water contact angle (WCA)

The change in surface wettability was characterized by the WCA measurements using the sessile drop technique. A droplet (1–1.5 μL) of ultrapure water was placed on the **(i)** non-coated **(ii)** nGel-coated **(iii)** Disinfection LT + HPGP (90 °C) **(iv)** Disinfection HT + Autoclave (134 °C) material surfaces, while the data points were taken by a contour monitor built in-house and the images were captured by MATLAB program.

2.8. Analysis of elemental composition by X-ray photoelectron spectroscopy (XPS)

The change in the surficial element composition of the **(i)** non-coated **(ii)** nGel-coated **(iii)** Disinfection LT + HPGP (90 °C) **(iv)** Disinfection HT + Autoclave (134 °C) materials was characterized by XPS. The XPS was conducted using an SSI S-Probe (Surface Science instrument, Mountain View, CA, USA) with a monochromatic Al Kα X-ray source (1486.8 eV). The pass energy was set at 150 eV for the survey spectra and the spectra was processed using the CasaXPS software (https://www.casaxps.com/). The reported binding energies are ± 0.1 eV and referenced to the C1*s* photoemission peak centered at a binding energy of 284.8 eV. Deconvolution of the spectra included a Shirley baseline subtraction and fitting with a minimum number of peaks consistent with the chemical structure of the sample, taking into account the experimental resolution. The profile of the peaks was taken as a convolution of Gaussian and Lorentzian functions. The uncertainty in the peak intensity determination is 2 % for all core levels reported.

2.9. Bacterial strain and growth conditions

S. aureus RN4220 was grown overnight at 37 °C on blood agar plate. The pre-culture was prepared by isolating a single colony of the bacteria using a sterilized loop and inoculated into 10 ml of tryptone soya broth (TSB; Oxoid, Basingstoke, UK). The suspension was vortexed to ensure proper mixing of the bacteria in TSB and stored in the incubator for 24 h at 37 °C. Afterwards, the previously made pre-culture was added to 200 ml of TSB main culture and incubated overnight. The main culture was centrifuged at 6500 rpm (5000 g) for 5 min at 10 °C, followed by washing and resuspension of the pellet in Phosphate buffer saline (PBS; 10 mM potassium phosphate, 0.15 M NaCl, maintained at pH ~ 7.4). In order to remove bacterial clusters, the PBS suspension was sonicated (Vibra Cell model VCX130; Sonics and Materials INC., Newtown, Connecticut, USA) in an ice bath for 30 s at 30 W. In the final stage, the bacterial count in the suspension was determined by the Bürker-Türk counting chamber and the bacterial concentration for further experiments were optimized accordingly.

2.10. Determination of bacterial attachment on sterilized nGel-coated surfaces- CFU method

The retention of function of the coated and sterilized surfaces were determined by enumerating the number of bacteria attached on the **(i)** non-coated and non-sterilized; **(ii)** coated and non-sterilized; **(iii)** coated and non-sterilized incubated in PBS (without bacteria); and **(iv)** coated and treated (different mode of D/S) surfaces by the CFU method. Bacterial concentration of $3x10^9$ bacteria/ml was suspended in PBS, and the materials were incubated in the bacterial suspension for 2 h at 24 °C to allow bacterial adhesion. Subsequently, the material surfaces were washed thrice with PBS to eliminate any poorly-attached bacteria and further, ultrasonicated in PBS for 30 s. After sonication, 1 ml of the detached bacterial suspension in PBS was pipetted and 10-fold serially diluted. In the following step, the diluted bacterial suspension was plated on TSB agar plate and incubated overnight at 37 °C before enumerating the CFU per ml.

2.11. Statistical analysis

All the experiments were performed thrice, independently. The statistical analysis for the enumeration experiment was conducted by 2-way analysis of variance (ANOVA) using the Dunnett test, keeping the coated, non-sterilized sample as the reference point for the wide range of D/S processes within each material. $p < 0.05$ was considered statistically significant in the analysis.

3. Results

3.1. nGel synthesis and particle characterization

NIPAM-*co*-APMA core shell nGel particles were synthesized by precipitation polymerization reaction with NIPAM as the primary monomer, APMA as co-monomer and BIS-acrylate as the cross-linker. After the initial reaction time, APMA was added into the turbid mixture of the nGel, which incorporated the primary amines (NH_2) to the periphery of the nGel shell. The positive charge of the amines in aqueous suspension ensures proper binding to the negatively-charged surfaces of the implant materials after plasma activation [28].

The temperature-dependent D_h determined by DLS was 510 nm at room temperature while, TEM indicated 406 nm diameter in the dry state. The volume phase transition temperature (VPTT) is seen at 33 °C according to the temperature-dependent DLS data, as shown in Fig. 1. The recorded zeta potential was + 13.5 ± 0.3 mV, which can be attributed to the presence of positively –NH_2 groups formed at the periphery on the nGel particles.

3.2. Formation, characterization, and sterilization of nGel coated implant materials

Eight different clinically-relevant implant materials were selected: PMMA, Teflon, PP, PEEK, Si-rubber, glass, titanium, and SS. Our group has previously reported this universal coating strategy employed to coat the materials in this study [28]. In brief, the materials were plasma oxidized to attain a negative charge on their surface, while the positively-charged NIPAM-*co*-APMA nGel particles were deposited on the implant surface via electrostatic interactions using a spray coating technique and were dried at 50 °C overnight. The surfaces were washed with ultrapure water for 6 h to remove any excess nGel and obtain a uniform monolayer, subsequently the nGel coated surfaces were characterized by AFM **(**Figs. 2 & 3**)**. The ellipsometry data was recorded with a laser of 632 nm at an incident angle of 65°. The thickness of the nGel coating layer on silicon wafer was ~70.6 nm, while the non-coated Si-wafer (control) was ~11.7 nm. The temperature-dependant property of the PNIPAM component of the coating is demonstrated with the WCA experiment. **Fig. S1** shows the change in WCA of the nGel coating on Teflon and SS measured at 24 °C and 50 °C beyond the VPTT. The coating at room temperature (24 °C) shows relatively lower WCA suggesting hydrophilic behavior of the particles in the coating, while the increase of WCA at 50 °C, indicates hydrophobic nature and collapsing of the particles beyond their VPTT [28,40]. This is also in accordance with the particle characterization method, temperature-dependant D_h measurements performed by DLS, as demonstrated in Fig. 1.

In order to assess the stability of the nGel coatings after the D/S processes, all the samples were characterized by AFM, before and after the D/S process indicating the optimum sterilization techniques for the diverse implant materials when applying the same nGel coating. The nGel coating stability on polymer and inorganic-based implant materials, after undergoing different sterilization methods was captured by AFM at room temperature, as represented in Fig. 2 (Polymeric materials) and Fig. 3 (Inorganic materials), respectively. Moreover, for better comparative study, AFM images of non-coated surfaces with or without sterilization are included in **Figs. S2** and **S3** to understand the effect of sterilization on these material surfaces, and whether potential coating damage is either due to the coating stability or alteration of the bulk material itself. This data is purely based on qualitative assessment, where uniform, homogenous coating that has remained intact post-D/S processes are considered as 'stable' coatings, while coatings that were partially/ completely washed away or showed any other defects (crack on the surface) are regarded as 'unstable' coatings. Figs. 2 and 3**(I–IV (a)),** shows the nGel-coated implant materials, without sterilization and they were compared to the AFM images of the implant materials after the IH and CR D/S techniques. From literature, it can already be assessed

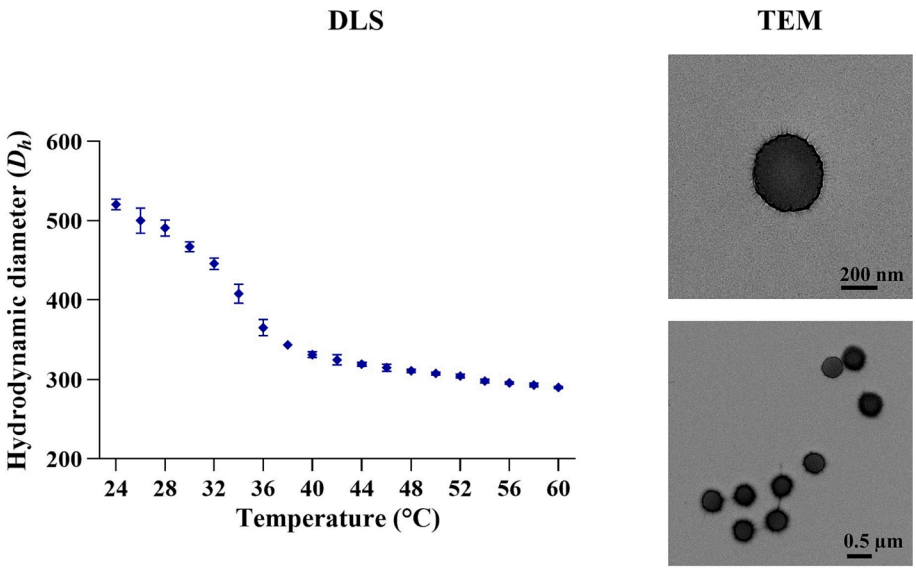

Fig. 1. Temperature-dependant D_h using DLS and TEM analysis of NIPAM-*co*-APMA nGel particles.

that PMMA has a low glass transition temperature (Tg), which is defined as the inherent property of a polymeric material at which it transforms from a glassy to rubbery state [41]. It is also non-autoclavable at 121 °C (Fig. 2**(Ib)**) and higher temperature, as its mechanical properties become affected [42]. Therefore, no data is shown for 134 °C, as it makes the material highly incompatible for clinical application, post-sterilization by autoclave. Fig. 2**(Ic)** shows swelling of the PMMA and the nGel coating on top of it. This is probably due to the penetration of the polar solvent (70 % ethanol) into the polymeric networks of PMMA, causing its transition from unsolvated glass to the solvated rubbery region and the change in volume [43–45]. As the coating on PMMA could not be observed, it was not considered for further experimental analysis. Teflon, PP, PEEK (Fig. 2**(II)**, **(III)** and **(IV)**, respectively) have displayed the best outcomes, where the nGel coating was stable, irrespective of the diverse D/S techniques. One of the key beneficial features of coatings is that the plasma adhesion layer modifies only the first few nanometers (nm) of the material, while the bulk of the material remains constant [46].

Non-hygroscopic material, such as Si-rubber is impermeable to the steam produced in autoclave [12], however, because the connecting layer is a thin oxide layer, the nGel coating was unstable and washed away (mostly), as captured by AFM and shown in Fig. 3**(Ib)** and **(Ie)**. Consequently, we did not proceed with further CR procedures for silicone, as these treatments were highly incompatible for the material. Fig. 3**II(b)** and **(h)** indicates an unstable coating on glass when treated by autoclave at 121 °C and 134 °C, which follows the same logic as surface oxidized silicone as both interfaces present an oxide layer. In case of titanium and SS, the coating was washed off when disinfected at LT (Fig. 3**(IIIe)** and **(IVe)**) and HT (Fig. 3**(IIIg)** and **(IVg)**), therefore further analysis for HPGP and at higher temperature was not taken into consideration. In **Tables S2 and S3**, we note that the average roughness (R_{avg}, nm) is greatly reduced when applying the nGel coating on all the surfaces, while they become slightly more rough, post D/S processes. The materials that present an unstable coating (either, 'completely washed away' or 'partly still remaining') contributed to the heightened increase in R_{avg}, as seen in PMMA autoclaved at 121 °C (changed from 19.2 nm for coated, before sterilization to 81.6 nm for coated after sterilization) or, titanium disinfected at LT and sterilized by HPGP (changed from 14.0 nm for coated, before sterilization to 44.6 nm for coated after sterilization). Glass is an exception to this as the R_{avg} of coated, autoclaved at 134 °C (1.72 nm) became comparable to the non-coated, autoclaved at 134 °C (1.90 nm) after the coating mostly washed away, as shown in Fig. 3**(IIh)**).

The AFM images of non-coated implant materials, with and without sterilization, are presented in **Figs. S2 and S3**. The complete overview of the coating stability on the nGel-coated implant materials after undergoing different D/S techniques is indicated in Table 1. Here, the coating is regarded as '✓' (stable) if no visual defects are seen in the AFM images, otherwise marked as '**X**'. The native roughness of the materials (prior to coating or any D/S methods) combined with added dimension after coating and sterilization, all contribute to the R_{avg} of the implant materials (**Tables S2 and S3**). The AFM data is further complemented with other surface characterization studies including the WCA (**Fig. S4**) and XPS (**Table S4**) to get an even better understanding on the effect of 2 clinically-relevant D/S techniques, Disinfection LT + HPGP (90 °C) and Disinfection HT + Autoclave (134 °C) on the NIPAM-*co*-APMA nGel coatings. For this, we considered **(a)** Teflon, **(b)** PP, **(c)** Si-rubber and **(d)** SS for the conditions **(i)** non-coated, **(ii)** nGel coated, **(iii)** Disinfection LT + HPGP (90 °C), and **(iv)** Disinfection HT + Autoclave (134 °C). A significant reduction in the WCA (**Fig. S4**) was observed from the non-coated to the nGel coated surfaces, owing to the surface coating for the increase in hydrophilicity [21,28]. Surfaces with intact coating after the D/S treatments showed comparable values of WCA with their corresponding nGel coated surfaces (in case of Teflon and PP), however, the WCA changed in Si-rubber and SS due to washing away of the major part of the surface coating. The XPS data indicated a marked increase in the atomic percentage of C1*s*, N 1*s*, and O 1*s*; coupled with a decrease in the F 1*s* content from the non-coated to the nGel coated Teflon surface (**Table S4(a)**), suggesting the presence of the coating. After the D/S treatments, the atomic percentage of C1*s*, N 1*s*, and O 1*s* remained comparable to the coated material, while a slight increase in the F 1 *s* content is noted. This could be due to the removal of a small portion of the coating. In the similar manner, an increment in the atomic percentage of C1*s*, N 1*s*, and O 1*s* along with reduction in Si 2*p* is observed when transitioning from non-coated to nGel coated Si-rubber surface (**Table S4(c)**). However, this gets reversed after the D/S treatments, where the Si 2*p* content increases resulting from the removal of the coating. Both the WCA and the XPS data are in accordance with the captured AFM images in Figs. 2 and 3.

3.3. Retention of antifouling function after sterilization of nGel coated implant materials

In addition to investigating the stability of the nGel coating, we also

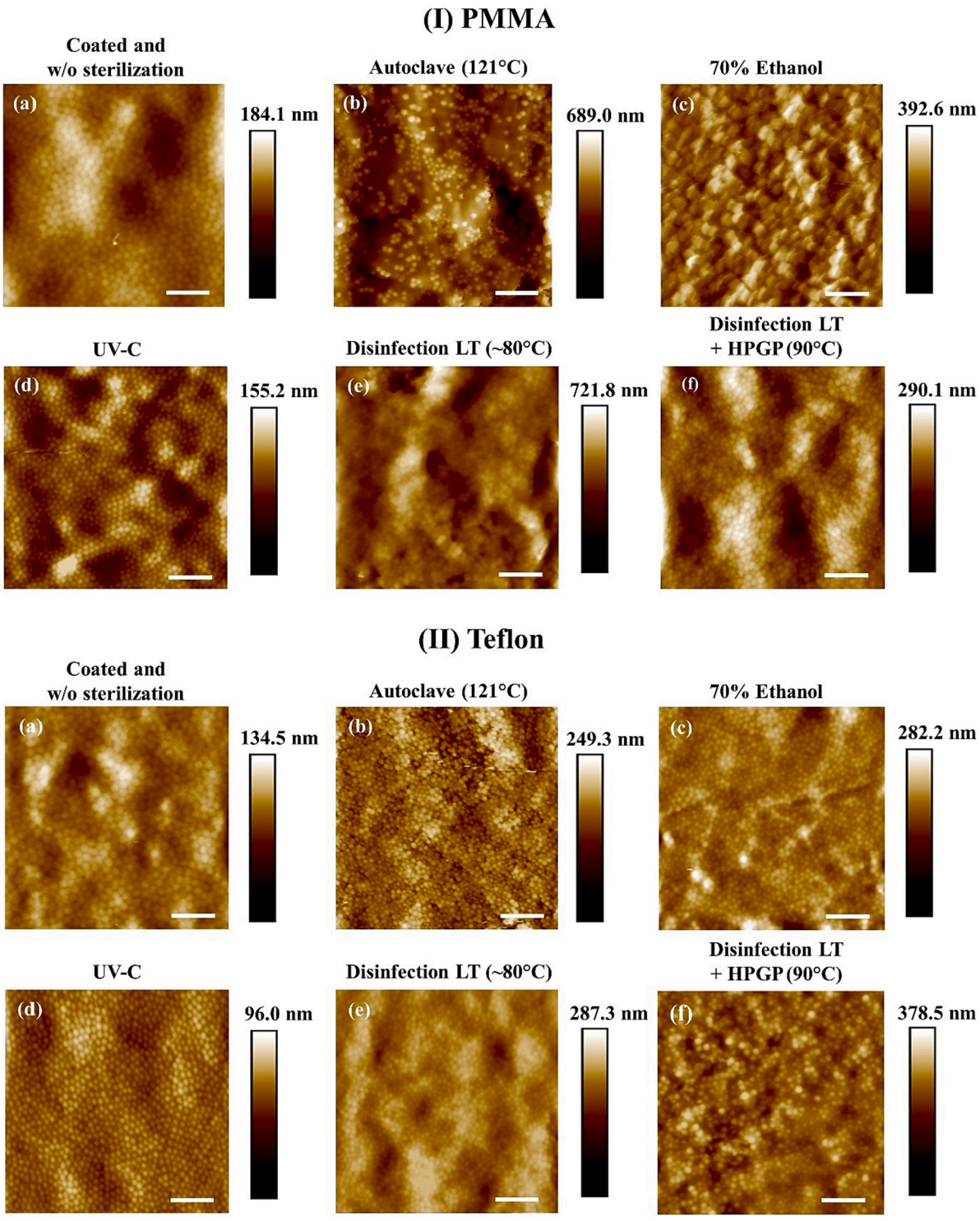

Fig. 2. AFM images captured at room temperature at a scanning area of (10x10) μm representing the nGel coating stability of polymer-based implant materials (PMMA, Teflon, PP and PEEK) on exposure to different IH (autoclave at 121 °C, 70 % ethanol and irradiated by UV-C) and CR (Disinfection at LT (~80 °C); Disinfection LT + sterilization by HPGP at 90 °C; Disinfection at HT (~115 °C); and Disinfection HT + sterilization by autoclave at 134 °C) techniques. Scale bar used 2 μm. (The lowest point on the height scale bar represents 0 nm).

assessed the retention of the antifouling function of the coating after the D/S processes. Only the 'coated and non-sterilized' materials were incubated in PBS (without bacteria; 1st control), while the 'non-coated and non-sterilized'; the 'coated and non-sterilized' (2nd control); and the 'coated and sterilized' materials were incubated in a bacterial suspension of *S.aureus* RN4220 for 2 h. Bacterial attachment was enumerated in terms of CFU/ml (in logarithm values), and illustrated in Fig. 4**(a)** polymeric and **(b)** inorganic materials. The quantitative data presented here is a comparative analysis between the treatment methods within the same coated material and their respective control group, ('coated and non-sterilized' material).

The 'non-coated, non-sterilized' polymeric and in-organic materials

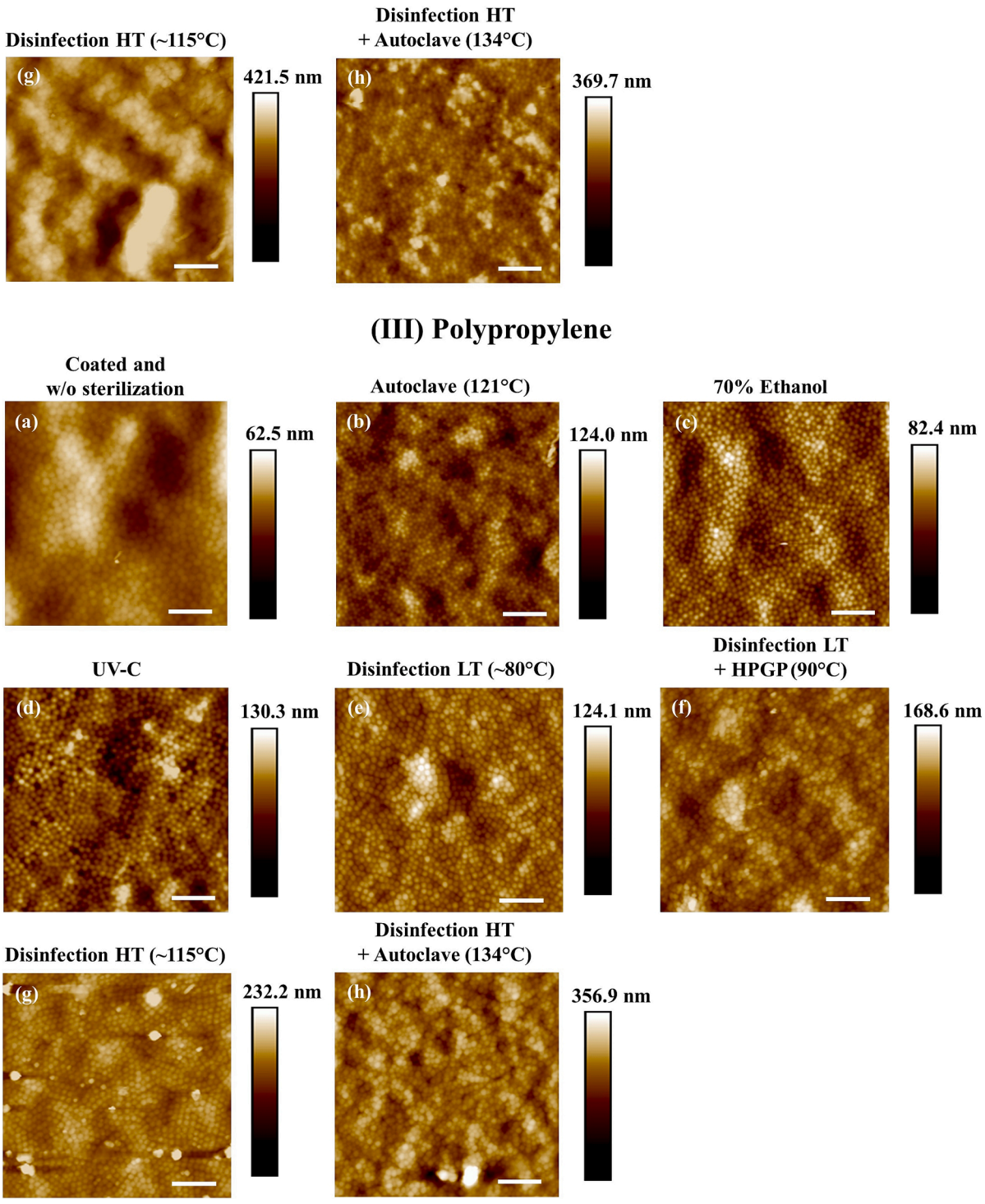

Fig. 2. (*continued*).

(Fig. 4**(a) and (b))** indicated larger number of bacterial colonies, in contrast to their control group of 'nGel coated, non-sterilized' for each material category. Comparative studies in antifouling experiments are generally performed between the 'non-coated and sterilized' group and the 'coated and sterilized group'. Here the inclusion of the intermediate category 'coated and non-sterilized' (marked as the 'black' bar in Fig. 4) has provided us with intriguing insights on influence of D/S approaches on the antifouling effect, in contrast to the 'coated and sterilized' groups. We immediately noted a significant reduction in bacterial adherence, which suggests lower bacterial adhesion due to the intrinsic nature of the nGels to form a hydration layer when coated, providing antifouling properties [31]. The 1st control, 'coated and non-sterilized' materials incubated in PBS (without any bacteria) was taken into account to check the presence of any bioburden (already existing bacteria) that might contribute to the number of adhered bacteria in each non-treated/ treated condition. No bacterial colonies were observed in undiluted (10^0) PBS solution, suggesting that the experiments were carried out aseptically and all the adhered bacteria were incorporated externally, therefore this group has not been represented in Fig. 4 and the Tryptone soya agar (TSA) plate (shown only for 'coated, non-sterilized' PEEK) is

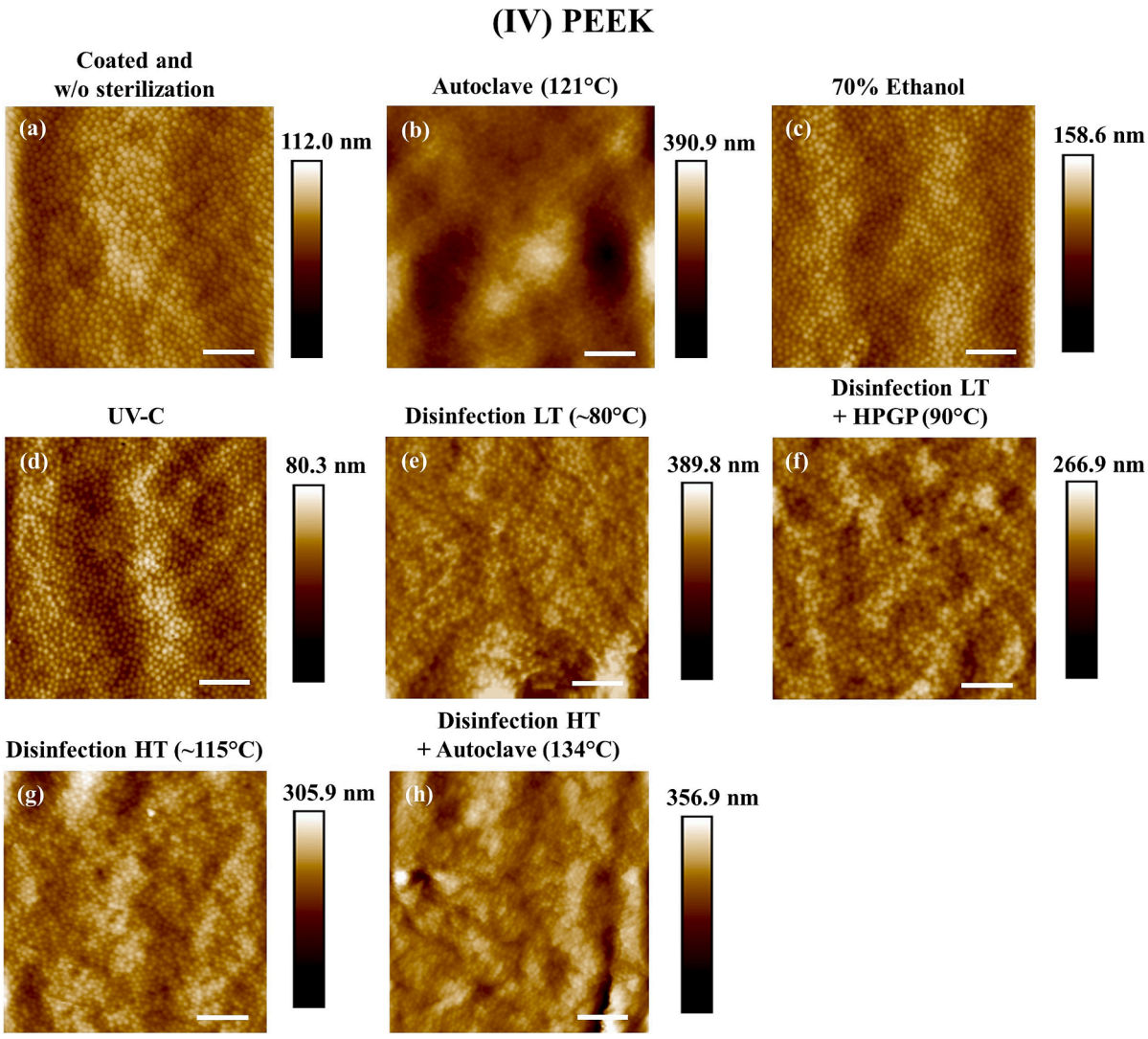

Fig. 2. (*continued*).

displayed in **Fig. S5**. Materials with 'already' compromised coating (as shown in Table 1 and depicted by AFM images in Figs. 2 and 3) such as PMMA disinfected by 70 % ethanol **(**Fig. 4**(a))** and glass autoclaved at 121 °C and 134 °C **(**Fig. 4**(b))** indicated heightened bacterial adhesion on the surface and assigned as '#' in the graph. Teflon, PP and PEEK in Fig. 4**(a)** showed retention of the antifouling function with respect to their 'coated, non-sterilized' control. Although the AFM image indicated a stable coating on glass after UV-C treatment, there is a loss of its antifouling function, while in materials like Si-rubber autoclaved at 121 °C, titanium, and SS sterilized by HPGP, the coating had partially washed away, marked as '#' **(**Fig. 4**(b))**, but these materials still exhibited low fouling (comparable to their corresponding control). Most likely on those surfaces there is still enough coating coverage left to remain functional. For instance, PEEK with stable coating exhibited 5.9 and 6.2 $log_{10}CFU/ml$ when disinfected with 70 % ethanol and autoclaved at 134 °C, respectively, while, glass displayed 6.4 and 6.8 $log_{10}CFU/ml$ of adhered bacteria, post treatment with 70 % ethanol and autoclave at 121 °C, respectively. Based on the Log_{10} *CFU/ml* data from Fig. 4, the percentage of bacteria still remaining on the implant surfaces, post-D/S techniques, was determined in Fig. 5**(a)**, while keeping the 'coated, non-sterilized' material as the reference group. Both of the factors- stability of the nGel coating (indicated in Table 1) and retention of the antifouling function after the D/S processes **(**Fig. 5**(a))** were combined in the overview table in Fig. 5**(b)**. Here, the coating was defined as 'good' if the coating is stable and shown close to 80 % (~*0.7* log) reduction in bacterial adhesion (20 % remaining), 'intermediate' for ≤ 66.6 % (*0.5* log) reduction (33.4 % remaining), while the rest were marked as 'inadequate' coatings after the nGel coated materials were treated by different D/S processes **(**Fig. 5**(b))**. As mentioned earlier, our group has demonstrated 98 % antifouling on coating negatively-charged NIPMAM particles on glass surface [37]. Keeping this data as our reference point, the combination of the nGel particle along with the type of implant material and the applied D/S technique; the status of 'good', 'intermediate' and 'inadequate' was designated in each case.

4. Discussion

A range of implant materials that are used in the clinic was considered for the D/S study. Post-sterilization, AFM images were captured of all the materials to visually determine the stability of the coating. 70 % ethanol is only a low-level primary disinfectant [11], so it does not find its applicability when considering implantation in the human body. Here, the data related to 70 % ethanol has been shown as it is an easy-to-use method and readily available disinfection technique and commonly used in the lab. A popular substitute to the already existing traditional D/S techniques was the use of HPGP. Although PMMA is non-autoclavable and has a low T_g, the coating indicated good stability when exposed to both disinfection at LT and disinfection LT +

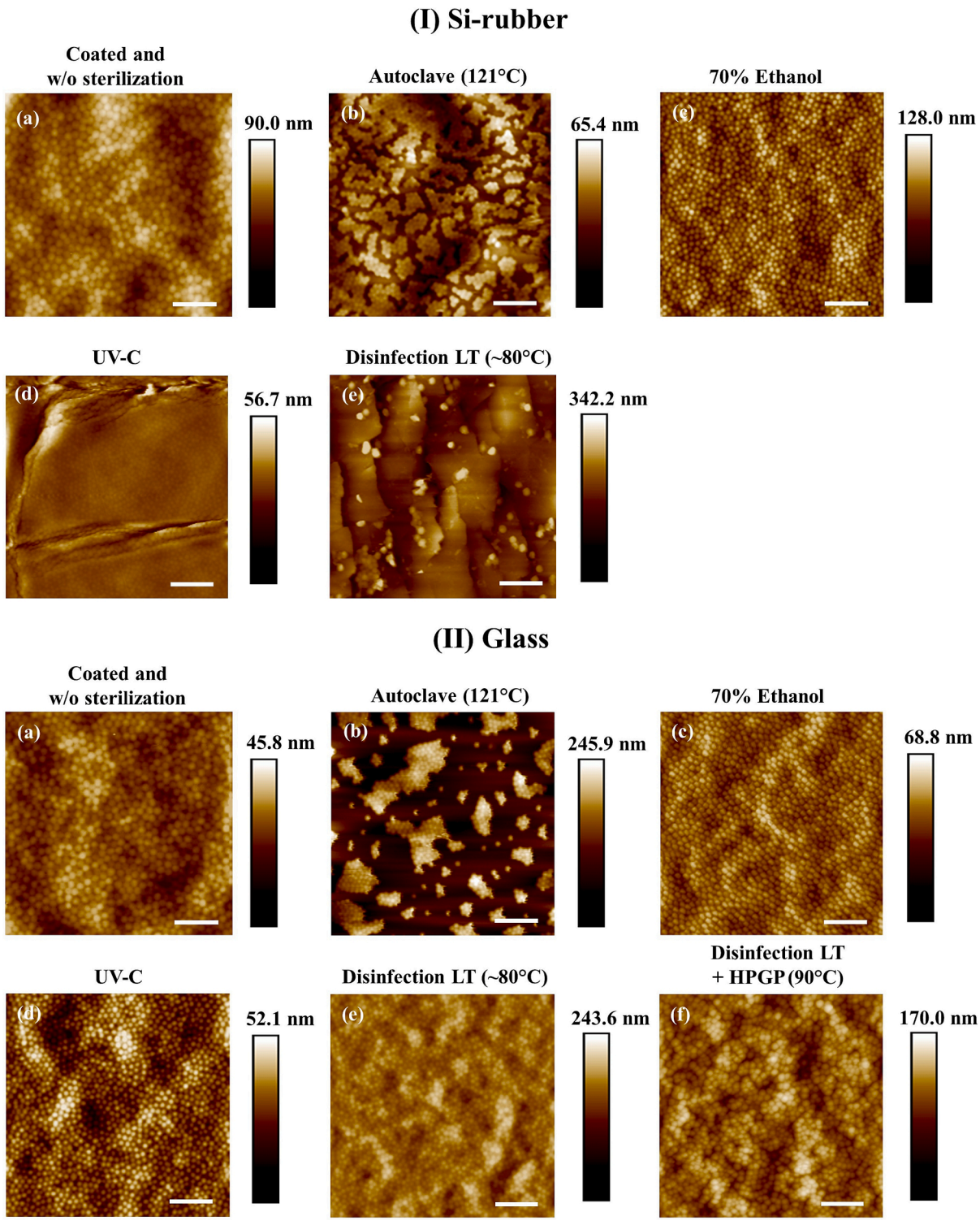

Fig. 3. AFM images captured at room temperature at a scanning area of (10x10) μm representing the nGel coating stability of inorganic-based materials (Si-rubber, Glass, Titanium and SS) materials on exposure to different IH (autoclave at 121 °C, 70 % ethanol and irradiated by UV-C) and CR (Disinfection at LT (~80 °C); Disinfection LT + sterilization by HPGP at 90 °C; Disinfection at HT (~115 °C); and Disinfection HT and sterilization by autoclave at 134 °C) techniques. Scale bar used 2 μm. (The lowest point on the height scale bar represents 0 nm).

sterilization by HPGP. The coating was stable on Teflon, PP, and PEEK, irrespective of the D/S techniques used. When irradiated with UV-C, the nGel-coated Si-rubber implant material underwent crosslinking, which causes hydroxylation and changes its chemical composition [47]. This resulted in embrittlement of the material and cracks were formed, as shown in Fig. 3**(Id)**. Successive cycles of steam sterilization (autoclave) of inorganic implant materials most likely dissolves the oxide layer (formed at the initial few nm of the material), [48] thereby disrupting the coating integrity on the material, as shown in AFM image (Fig. 3**)**. Titanium and its alloys are corrosion resistant materials, which is a key

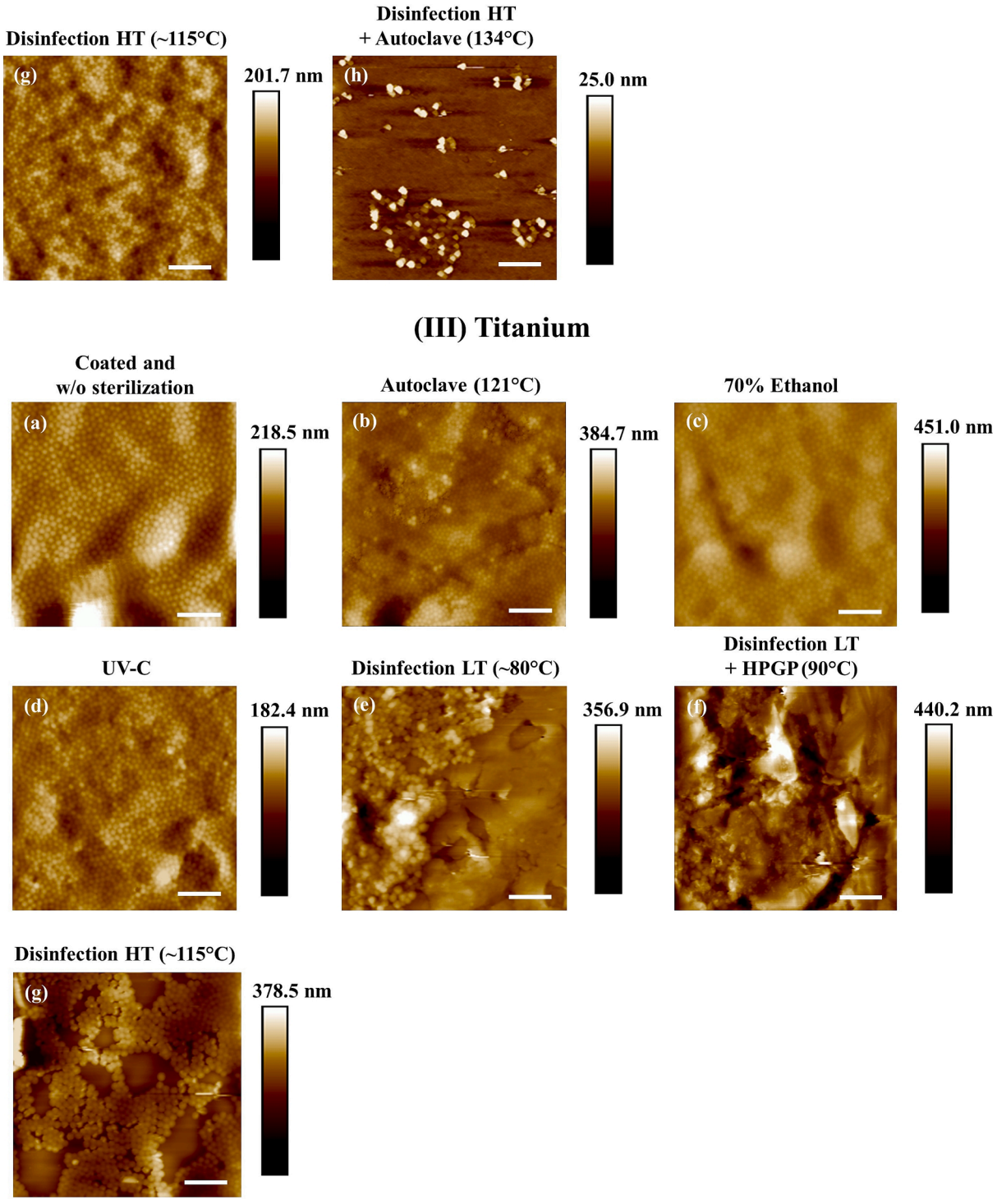

Fig. 3. (*continued*).

feature for medical implant materials [49], however, treatment with corrosive HPGP can degrade the metal to some extent [50], causing poor stability of the nGel coating on the surface, as shown in the AFM image (Fig. 3**III (e)** and **(f)**). Zirconium is widely used as dental implants [51] and does not undergo catalytic degradation when exposed to sterilization by HPGP [50]. A potential alternative to the conventional metal implants is the use of a polymeric implant, PEEK, for orthopedic implants, dental prostheses, cranial and maxillo-facial surgery, or cartilage replacement after injury [52,53]. This semi-crystalline thermoplastic polymer has outstanding thermal stability at HT thus, exhibits high T_g. It is resistant to hydrolysis or the effects of ionizing radiation and expresses low inflammatory response, while the mechanical strength can be further reinforced by incorporating organic or inorganic composites [54–56].

Both coating stability and the retention of function (here, anti-fouling) of the nGel coating, post-sterilization are equally important components when considering the applicability of the implant materials in clinical settings. Various physical factors like change in surface roughness, surrounding temperature (our focus in this research), wettability, charge interactions, surface energy, and chemical

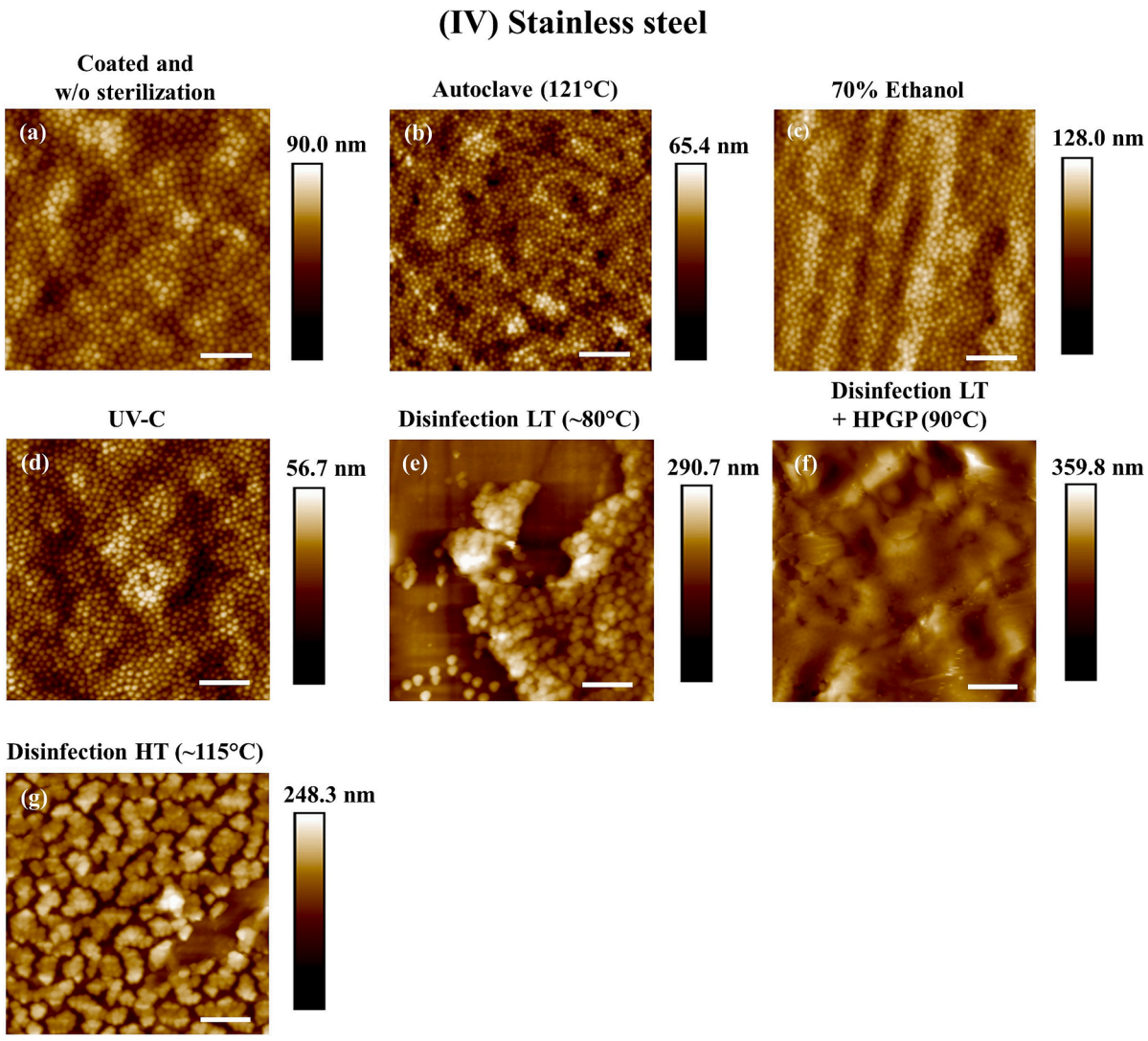

Fig. 3. (*continued*).

Table 1
Overview of coating integrity on the nGel-coated implant surfaces after undergoing different disinfection/ sterilization processes. The '✓' and '**X**' indicate the stability of the coating on the implant surface based on AFM images in Figs. 2 and 3. The coating is regarded as '✓' (stable) if the AFM images indicated the presence of a complete intact homogenous nGel coating (without any voids that are not covered with nGel), otherwise marked as '**X**'.

	Autoclave (121 °C)	70 % ethanol	UV-C radiation	Disinfection (LT)	Disinfection (LT) + HPGP (90 °C)	Disinfection (HT)	Disinfection (HT) + autoclave (134 °C)
PMMA	x	x	✓	✓	✓	x	x
Teflon	✓	✓	✓	✓	✓	✓	✓
PP	✓	✓	✓	✓	✓	✓	✓
PEEK	✓	✓	✓	✓	✓	✓	✓
Si-rubber	x	✓	x	x	x	x	x
Glass	x	✓	✓	✓	✓	✓	x
Titanium	x	✓	✓	x	x	x	x
SS	✓	✓	✓	x	x	x	x

composition play a major role in bacterial adherence after exposure to different treatment methods [57]. However, our observation from Fig. 4 was that in many cases, the antifouling behavior of the nGel coated implant materials was enhanced after undergoing the D/S techniques. The NIPAM particles, being thermosensitive by nature, undergo swelling or shrinking below and above its VPTT, respectively. The VPTT of NIPAM-*co*-APMA particles is at 33 °C (Fig. 1) however, on interaction with organic solvents like 70 % ethanol, the VPTT shifts to a lower temperature than the temperature in pure water, here 33 °C. This is explained by the co-nonsolvency effect [58–61] and thus, the nGel particles in the coating already collapses at room temperature. Other D/S processes such as UV-C, autoclaving, and HPGP involve the generation of heat, where the temperature rises above the VPTT. All these events flatten the particles and enhances contact with the surface. When the nGel-coating returns to room temperature, they cannot recover to their initial spherical structure as they have 'already' attached to the material

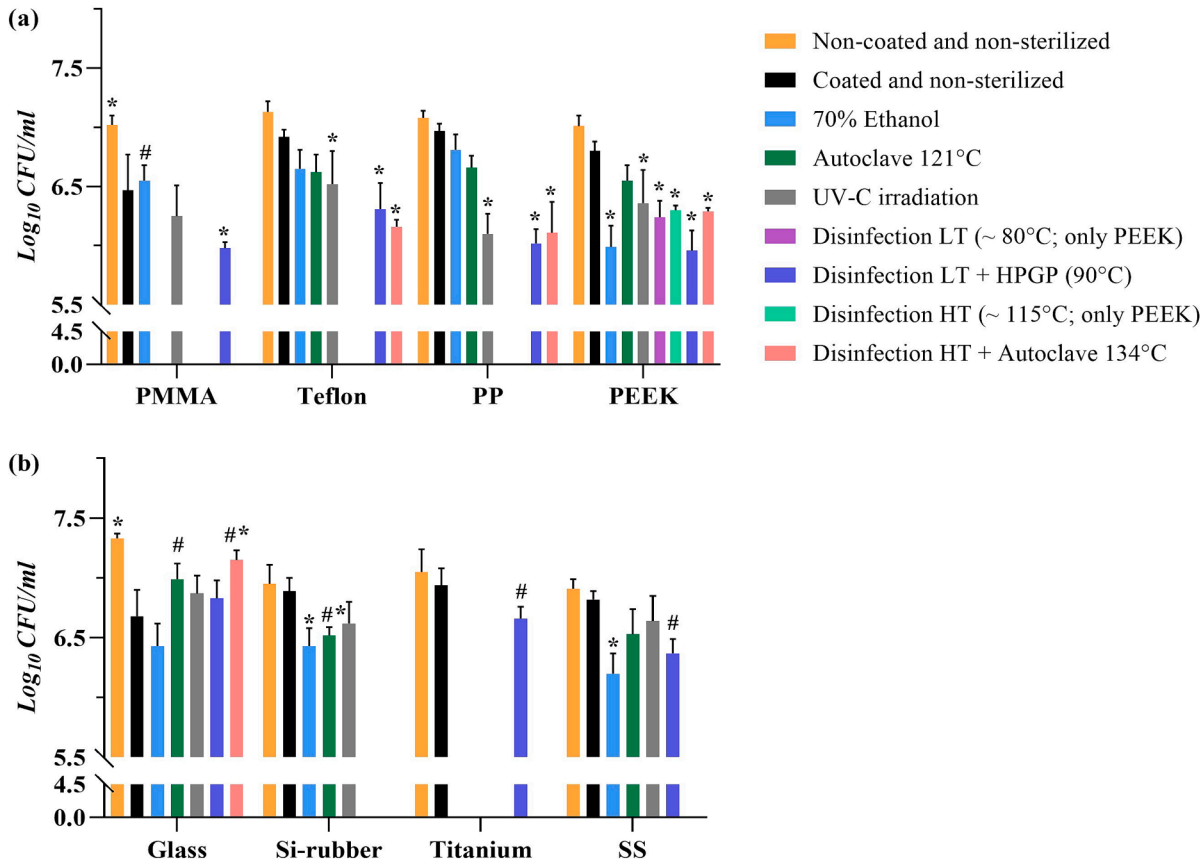

Fig. 4. *Log_{10} CFU/ml* to enumerate the number of adhered *S. aureus* RN4220 after 2 h incubation in bacterial suspension to determine the integrity of the antifouling function on the **(i)** non-coated and non-sterilized; **(ii)** nGel-coated and non-sterilized and **(iii)** nGel-coated and sterilized **(a)** polymeric **(b)** in-organic implant materials by different D/S techniques. All results are shown with respect to the 'coated, non-sterilized' samples in each case. Samples with 'already' unstable nGel coating are indicated by '#'. All the bacterial cultures, coatings and experiments were conducted three independent times. 2-way ANOVA was performed using the Dunnett test and the statistically significant differences, $p < 0.05$ are denoted by *. The standard deviation is marked by the error bars (n = 3).

surface and remain at the surface at higher density/more closed-packed coverage [62–64]. This re-packing intensifies the overall antifouling function of the materials, when referenced with their coated, non-sterilized counterpart (Fig. 4**(a) and (b)**). This phenomenon was further illustrated by placing 'nGel coated, non-sterilized' Si-rubber materials in bacterial suspension at 24 °C and 40 °C (**Fig. S6(a)**) to enumerate the difference in bacterial attachment (or, the extent of antifouling) at the two given temperatures by *log_{10}CFU/ml* (**Fig. S6(b)**). The coating was additionally characterized by AFM when the nGel particles returned to room temperature (**Fig. S6(c)**). The results show that indeed bringing the coating above the VPPT before use enhances the nGel antifouling behavior as the CFU count was lower for the heat-treated samples. The polymeric implant materials presented with stable antifouling function, with special mention to PP and PEEK for their exceptional ability to tolerate most CR D/S processes in the context of both coating stability (Fig. 2**(IV)**) and retention of the antifouling function, (Fig. 4**(a)**) making them a highly robust material of choice.

The interplay among the three crucial factors- implant material, nGel coating (with specific function), and the applied D/S processes; form the pillars behind the fate (success or failure) of the implant for clinical translation/ application. It should be noted that here the designation of 'good', 'intermediate' or 'inadequate' coating is only confined to our use of type of materials, nGel, and the treatment combinations, while part of the study still have to be repeated or redesigned on altering any of the three pillars. Keskin et al. has demonstrated a 98 % (*~1.5* log) reduction (only 2 % bacteria remaining) in bacterial attachment on the negatively charged P(NIPMAM) nGel coated glass material [37]. In our previous work where we developed a universal nanogel-based coating approach for medical implant materials, we have successfully demonstrated the application of the positively-charged NIPAM-*co*-APMA nanogel (nGel) particles for coating 11 distinct materials with different physicochemical properties [28]. The coating was homogenous and stable in both *in vitro* and short term *in vivo* study and therefore, we developed a truly universal coating strategy. D/S form a crucial part of research when considering to progress towards clinical relevance. Therefore, as part of our already established system and continuation of our previous work, we have studied the same nGel coating (while, implementing the same coating approach) to understand the effect of sterilisation on the nGel-based universal coatings.

As indicated that the primary amines based nGels particles are positively-charged so the proteins and polysaccharides being negatively-charged will attach to the coating via electrostatic interactions. It is important to understand that here we have presented the most aggressive/ extreme conditions (in terms of choice of particles and treatment methods) and the nGel based coatings still indicate an improvement in the antifouling activity for the surfaces with stable coating after the D/S techniques. This also suggests that if negatively-charged NIPAM or NIPMAM-based coatings are used, then the antifouling behavior will show tremendous improvement [37]. While the positively-charged NIPAM-*co*-APMA nGel particle is not the most optimum choice to investigate for antifouling function, our focus here is to study the retainability of the innate antifouling function in the nGel, following the treatment with different D/S procedures. Following this, our research also gives an indication of the possibility to retain any other functions post sterilization in the future.

Some points of discussion that remains is the possibility of sterilizing

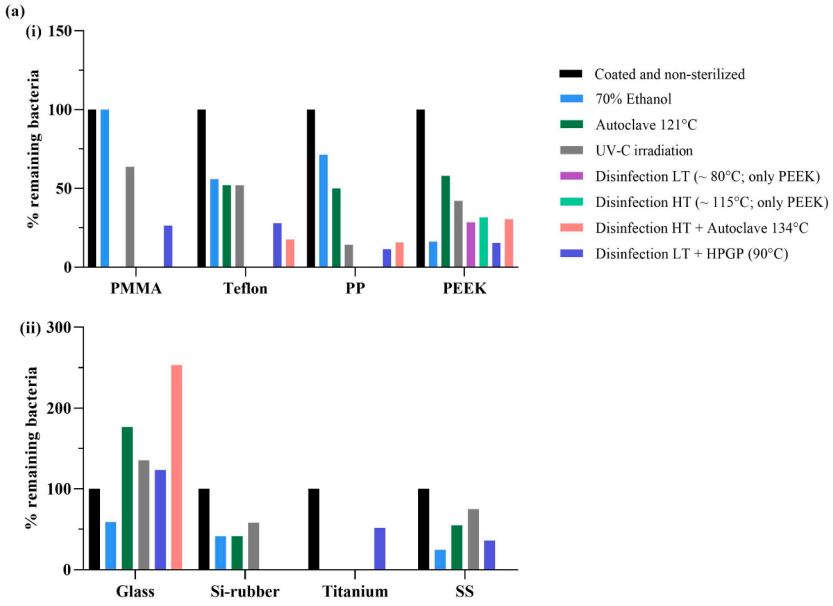

(b)

	Autoclave (121°C)	70% ethanol	UV-C radiation	Disinfection (LT)	Disinfection (LT) + HPGP (90°C)	Disinfection (HT)	Disinfection (HT) + autoclave (134°C)
PMMA	X	X	X		-		X
Teflon	X	X	X		-		+
PP	X	X	+		+		+
PEEK	X	+	X	-	+	-	-
Si-rubber	X	X	X		X		X
Glass	X	X	X		X		X
Titanium	X	X	X		X		X
SS	X	-	X		X		X

Fig. 5. **(a)** Percentage of bacteria remaining on the nGel-coated implant surfaces after D/S processes, compared to their corresponding 'nGel-coated, non-sterilized' implant materials (control), calculated from Log_{10} *CFU/ml* data in Fig. 4 **(b)** Overview of 'good' (denoted as '+'); intermediate (denoted as '-'); and 'inadequate' coating (denoted as '**X**') both in terms of stability and retention of the antifouling function on nGel-coated implant surfaces with the potential for clinical suitability/applicability (based on the quantitative data obtained from **(a)**). Along with the coating stability data from Table 1, it is regarded as 'good' at close to 80 % (~*0.7* log) bacterial reduction (20 % remaining), 'intermediate' is marked for ≤ 66.6 % (*0.5* log) reduction (33.4 % remaining), and the rest of the conditions were regarded as 'inadequate' coatings. The antifouling study for Disinfection LT and HT was only performed for PEEK, so the entries for the other materials is kept blank.

the implant materials prior to coating and implantation in an aseptic environment. The coating strategy demonstrated here is simple, easy to implement, cost and time-effective. Therefore, if the coating technology can be integrated within the clinical setting, consequently, the question of the stability of the coating and the sustenance of the function along with it can be addressed even better. Additionally, when considering clinal translation, it is of paramount importance to address the issue of storage and implementation of the thermosensitive coatings in the physiological system. Based on the VPTT of NIPAM-*co*-APMA nGel coatings, it is preferable to store them at body temperature (above the

VPTT at 33 °C), where the particles are in their hydrophobic state. This would also mean that during its real-time application in the body, the particles do not undergo any change in their size or the extent of wettability. However, this subject should be revisited on altering any of the aforementioned pillars responsible for the fate of the implant in the body. For instance, if NIPAM or NIPMAM-based coatings are used, then their respective VPTT would also change (shift) and the storage temperature should be reconsidered. While these *in vitro* data are promising, additional *in vivo* studies would provide more conclusive results on the effect of different sterilization techniques on the coating integrity and stability of other functionalities such as antimicrobial, antifouling [29], encapsulated drugs/ drug release [31] or imaging modalities [34].

5. Conclusions

Medically-relevant implant materials belonging to different classes of implants were examined with and without the NIPAM-*co*-APMA nGel coating and they underwent a versatile range of IH and CR D/S techniques. The polymeric materials showed stable coating under most D/S processes, while the coating washed away after treatment of the inorganic materials. The combination of the implant material used, type of nGel applied as coating and the D/S method used play a role in guiding the clinical success or failure of the implant in the host body. While our research indicates a high reduction in the adherence of bacteria on the 'nGel coated, sterilized' PP and PEEK, it is only specific to these conditions. Changing any of these factors would require a part of the study to be repeated again. The study is of utmost importance when considering the translation of bench research to clinical applications. Our research provides a thorough overview of the optimum D/S techniques (though, gamma irradiation and ethylene oxide were not considered here) that are compatible to the implant materials and furthermore, provide an indication for the possibility to sterilize other functionalized (drug, antimicrobials, imaging modalities) nGel coated implant materials in the future.

CRediT authorship contribution statement

Devlina Ghosh: Data curation, Formal analysis, Investigation, Methodology, Writing – original draft. **Brandon W. Peterson:** Data curation, Methodology. **Cees de Waal:** Data curation, Methodology. **Joop de Vries:** Data curation, Methodology. **Hans Kaper:** Data curation, Methodology. **Guangyue Zu:** Data curation, Methodology. **Max Witjes:** Conceptualization, Supervision, Writing – review & editing. **Patrick van Rijn:** Conceptualization, Funding acquisition, Resources, Supervision, Writing – review & editing.

Declaration of competing interest

The authors declare that they have no known competing financial interests or personal relationships that could have appeared to influence the work reported in this paper.

Data availability

Data will be made available on request.

Acknowledgements

All the authors acknowledge the financial support of the Graduate School of Medical Sciences (GSMS) of University Medical Centre of Groningen, the Netherlands and the China Scholarship Council (CSC no.201706890012). The authors also thank the support of SteriNoord BV, Groningen, the Netherlands for their immense contribution in giving us access to the clinically-relevant sterilization techniques and Willem Woudstra for discussions related to the antifouling experiments.

Appendix A. Supplementary data

Supplementary data to this article can be found online at https://doi.org/10.1016/j.matdes.2024.112689.

References

[1] Y. Mehta, A. Gupta, S. Todi, S.N. Myatra, D.P. Samaddar, V. Patil, P. K. Bhattacharya, S. Ramasubban, Guidelines for prevention of hospital acquired infections, Indian J. Crit. Care Med. 18 (2014) 149, https://doi.org/10.4103/0972-5229.128705.
[2] M.B. Edmond, R.P. Wenzel, Infection Prevention in the Health Care Setting, Mand. Douglas, Bennett's Princ. Pract. Infect. Dis. 2 (2015) 3286. https://doi.org/10.1016/B978-1-4557-4801-3.00300-3.
[3] H.A. Khan, F.K. Baig, R. Mehboob, Nosocomial infections: Epidemiology, prevention, control and surveillance, Asian Pac, J Trop. Biomed. 7 (2017) 478–482, https://doi.org/10.1016/J.APJTB.2017.01.019.
[4] T. Kärki, D. Plachouras, A. Cassini, C. Suetens, K. Latour, E.-R. Ricchizzi, P. Kinross, M.L. Moro, Burden of healthcare-associated infections in European acute care hospitals, Wiener Medizinische Wochenschrift 1691 (169) (2019) 3–5, https://doi.org/10.1007/S10354-018-0679-2.
[5] G. Panta, A.K. Richardson, I.C. Shaw, Effectiveness of autoclaving in sterilizing reusable medical devices in healthcare facilities, J. Infect. Dev. Ctries. 13 (2019) 858–864, https://doi.org/10.3855/JIDC.11433.
[6] S. Szabó, B. Feier, D. Capatina, M. Tertis, C. Cristea, A. Popa, An Overview of Healthcare Associated Infections and Their Detection Methods Caused by Pathogen Bacteria in Romania and Europe, J. Clin. Med. 2022, Vol. 11, Page 3204. 11 (2022) 3204. https://doi.org/10.3390/JCM11113204.
[7] W.A. Rutala, D.J. Weber, Disinfection and sterilization in health care facilities: an overview and current issues, Infect. Dis. Clin. North Am. 30 (2016) 609, https://doi.org/10.1016/J.IDC.2016.04.002.
[8] E.A. Gonzalez, P. Nandy, A.D. Lucas, V.M. Hitchins, Ability of cleaning-disinfecting wipes to remove bacteria from medical device surfaces, Am. J. Infect. Control. 43 (2015) 1331–1335, https://doi.org/10.1016/J.AJIC.2015.07.024.
[9] J.H. Park, R. Olivares-Navarrete, R.E. Baier, A.E. Meyer, R. Tannenbaum, B. D. Boyan, Z. Schwartz, Effect of cleaning and sterilization on titanium implant surface properties and cellular response, Acta Biomater. 8 (2012) 1966–1975, https://doi.org/10.1016/j.actbio.2011.11.026.
[10] S. Mohapatra, Sterilization and Disinfection, Essentials of Neuroanesthesia. (2017) 929, https://doi.org/10.1016/B978-0-12-805299-0.00059-2.
[11] M.U. Graziano, K.U. Graziano, F.M.G. Pinto, C.Q. de M. Bruna, R.Q. de Souza, C. A. Lascala, Effectiveness of disinfection with alcohol 70% (w/v) of contaminated surfaces not previously cleaned, Rev. Lat. Am. Enfermagem. 21 (2013) 618–623, https://doi.org/10.1590/S0104-11692013000200020.
[12] W.J. Rogers, Steam and dry heat sterilization of biomaterials and medical devices, Sterilisation Biomater. Med. Devices. (2012) 20–55, https://doi.org/10.1533/9780857096265.20.
[13] G. McDonnell, The use of hydrogen peroxide for disinfection and sterilization applications, PATAI'S Chem. Funct. Groups. (2014) 1–34, https://doi.org/10.1002/9780470682531.PAT0885.
[14] M. Buonanno, M. Stanislauskas, B. Ponnaiya, A.W. Bigelow, G. Randers-Pehrson, Y. Xu, I. Shuryak, L. Smilenov, D.M. Owens, D.J. Brenner, 207-nm UV light - a promising tool for safe low-cost reduction of surgical site infections. II: In-vivo safety studies, PLoS One. 11 (2016), https://doi.org/10.1371/journal.pone.0138418.
[15] T. Dai, M.S. Vrahas, C.K. Murray, M.R. Hamblin, Ultraviolet C irradiation: an alternative antimicrobial approach to localized infections? Expert Rev. Anti. Infect. Ther. 10 (2012) 185, https://doi.org/10.1586/ERI.11.166.
[16] V. Vignali, T. Hoff, J. de Vries-Idema, dr Anke Huckriede, dr Jan Maarten van, P. van Rijn, An efficient UV-C disinfection approach and biological assessment strategy for microphones, MedRxiv. (2022), https://doi.org/10.1101/2022.07.09.22277021.
[17] E. Laneve, B. Raddato, M. Dioguardi, G. Di Gioia, G. Troiano, L. Lo Muzio, Sterilisation in dentistry: a review of the literature, Int. J. Dent. (2019), https://doi.org/10.1155/2019/6507286.
[18] B.J. Parsons, Sterilisation of healthcare products by ionising radiation: principles and standards, Sterilisation Biomater. Med. Devices. (2012) 56–70, https://doi.org/10.1533/9780857096265.56.
[19] M. Molina, M. Asadian-Birjand, J. Balach, J. Bergueiro, E. Miceli, M. Calderón, Stimuli-responsive nanogel composites and their application in nanomedicine, Chem. Soc. Rev. 44 (2015) 6161–6186, https://doi.org/10.1039/c5cs00199d.
[20] Y. Sasaki, K. Akiyoshi, Nanogel engineering for new nanobiomaterials: from chaperoning engineering to biomedical applications, Chem. Rec. 10 (2010) n/a-n/a, https://doi.org/10.1002/tcr.201000008.
[21] D. Keskin, G. Zu, A.M. Forson, L. Tromp, J. Sjollema, P. van Rijn, Nanogels: a novel approach in antimicrobial delivery systems and antimicrobial coatings, Bioact. Mater. 6 (2021) 3634–3657, https://doi.org/10.1016/j.bioactmat.2021.03.004.
[22] Y. Yin, B. Hu, X. Yuan, L. Cai, H. Gao, Q. Yang, Nanogel: a versatile nano-delivery system for biomedical applications, Pharmaceutics. 12 (2020), https://doi.org/10.3390/pharmaceutics12030290.
[23] J. Yin, D. Dupin, J. Li, S.P. Armes, S. Liu, pH-induced deswelling kinetics of sterically stabilized poly(2-vinylpyridine) microgels probed by stopped-flow light scattering, Langmuir. 24 (2008) 9334–9340, https://doi.org/10.1021/la8014282.

[24] H. Kobayashi, R. Halver, G. Sutmann, R.G. Winkler, Polymer conformations in ionic microgels in the presence of salt: theoretical and mesoscale simulation results, Polymers (basel). 9 (2017), https://doi.org/10.3390/POLYM9010015.
[25] S. Schimka, Y.D. Gordievskaya, N. Lomadze, M. Lehmann, R. Von Klitzing, A. M. Rumyantsev, E.Y. Kramarenko, S. Santer, Communication: light driven remote control of microgels' size in the presence of photosensitive surfactant: complete phase diagram, J. Chem. Phys. 147 (2017) 031101, https://doi.org/10.1063/1.4986143.
[26] T.E. De Oliveira, P.A. Netz, D. Mukherji, K. Kremer, Why does high pressure destroy co-non-solvency of PNIPAm in aqueous methanol? Soft Matter. 11 (2015) 8599–8604, https://doi.org/10.1039/C5SM01772F.
[27] V. Audonnet, L. Malaquin, J.L. Viovy, Polymeric coatings on micro- and nanometric particles for bioapplications, Bioanal. Rev. 3 (2011) 41–66, https://doi.org/10.1007/s12566-011-0022-5.
[28] D. Ghosh, D. Keskin, A.M. Forson, C.W.K. Rosman, R. Bron, C.M. Siebenmorgen, G. Zu, A. Lasorsa, P.C.A. Van, D. Wel, T.G. Van Kooten, M.J.H. Witjes, J. Sjollema, H.C. Van, D. Mei, P. Van Rijn, A universal nanogel-based coating approach for medical implant materials, Adv. Nanobiomed Res. (2023) 2200141, https://doi.org/10.1002/ANBR.202200141.
[29] I. Francolini, C. Vuotto, A. Piozzi, G. Donelli, Antifouling and antimicrobial biomaterials: an overview, APMIS. 125 (2017) 392–417, https://doi.org/10.1111/APM.12675.
[30] O. Sójka, H.C. van der Mei, P. van Rijn, M.C. Gagliano, Zwitterionic poly (sulfobetaine methacrylate)-based hydrogel coating for drinking water distribution systems to inhibit adhesion of waterborne bacteria, Front. Bioeng. Biotechnol. 11 (2023), https://doi.org/10.3389/FBIOE.2023.1066126/FULL.
[31] D. Keskin, L. Tromp, O. Mergel, G. Zu, E. Warszawik, H.C. van der Mei, P. van Rijn, Highly efficient antimicrobial and antifouling surface coatings with triclosan-loaded nanogels, ACS Appl. Mater. Interfaces. 12 (2020) 57721–57731, https://doi.org/10.1021/acsami.0c18172.
[32] L. Ribovski, E. de Jong, O. Mergel, G. Zu, D. Keskin, P. van Rijn, I.S. Zuhorn, Low nanogel stiffness favors nanogel transcytosis across an in vitro blood–brain barrier, nanomedicine nanotechnology, Biol. Med. 34 (2021) 102377, https://doi.org/10.1016/j.nano.2021.102377.
[33] G. Zu, O. Mergel, L. Ribovski, R. Bron, I.S. Zuhorn, P. Rijn, Nanogels with selective intracellular reactivity for intracellular tracking and delivery, Chem. – A Eur. J. 26 (2020) 15084–15088, https://doi.org/10.1002/chem.202001802.
[34] G. Zu, Y. Cao, J. Dong, Q. Zhou, P. van Rijn, M. Liu, R. Pei, Development of an aptamer-conjugated polyrotaxane-based biodegradable magnetic resonance contrast agent for tumor-targeted Imaging, ACS Appl. Bio Mater. 2 (2019) 406–416, https://doi.org/10.1021/acsabm.8b00639.
[35] S. Mohammadi, H. Ravanbakhsh, S. Taheri, G. Bao, L. Mongeau, Immunomodulatory microgels support proregenerative macrophage activation and attenuate fibroblast collagen synthesis, Adv. Healthc. Mater. 11 (2022) 2102366, https://doi.org/10.1002/ADHM.202102366.
[36] P. Saha, R. Ganguly, X. Li, R. Das, N.K. Singha, A. Pich, Zwitterionic nanogels and microgels: an overview on their synthesis and applications, Macromol. Rapid Commun. 42 (2021) 2100112, https://doi.org/10.1002/MARC.202100112.
[37] D. Keskin, O. Mergel, H.C. Van Der Mei, H.J. Busscher, P. Van Rijn, Inhibiting bacterial adhesion by mechanically modulated microgel coatings, Biomacromolecules. 20 (2019) 243–253, https://doi.org/10.1021/acs.biomac.8b01378.
[38] O. Sójka, D. Keskin, H.C. van der Mei, P. van Rijn, M.C. Gagliano, Nanogel-based coating as an alternative strategy for biofilm control in drinking water distribution systems, Biofouling. (2023), https://doi.org/10.1080/08927014.2023.2190023/SUPPL_FILE/GBIF_A_2190023_SM7334.PDF.
[39] V. Damle, K. Wu, O. De Luca, N. Ortí-Casañ, N. Norouzi, A. Morita, J. de Vries, H. Kaper, I.S. Zuhorn, U. Eisel, D.E.P. Vanpoucke, P. Rudolf, R. Schirhagl, Influence of diamond crystal orientation on the interaction with biological matter, Carbon N. Y. 162 (2020) 1–12, https://doi.org/10.1016/J.CARBON.2020.01.115.
[40] P. Liu, M. Freeley, A. Zarbakhsh, M. Resmini, Adsorption of soft NIPAM nanogels at hydrophobic and hydrophilic interfaces: conformation of the interfacial layers determined by neutron reflectivity, J. Colloid Interface Sci. 623 (2022) 337–347, https://doi.org/10.1016/J.JCIS.2022.05.010.
[41] M. Mohammadi, J. Davoodi, M. Javanbakht, H. Rezaei, Glass transition temperature of PMMA/modified alumina nanocomposite: molecular dynamic study, Mater. Res. Express. 6 (2018) 035309, https://doi.org/10.1088/2053-1591/AAF6D5.
[42] T.J.A.G. Münker, S.E.C.M. van de Vijfeijken, C.S. Mulder, V. Vespasiano, A. G. Becking, C.J. Kleverlaan, A.G. Becking, L. Dubois, L.H.E. Karssemakers, D.M. J. Milstein, S.E.C.M. van de Vijfeijken, P.R.A.M. Depauw, F.W.A. Hoefnagels, W. P. Vandertop, C.J. Kleverlaan, T.J.A.G. Münker, T.J.J. Maal, E. Nout, M. Riool, S.A. J. Zaat, Effects of sterilization on the mechanical properties of poly(methyl methacrylate) based personalized medical devices, J. Mech. Behav. Biomed. Mater. 81 (2018) 168–172, https://doi.org/10.1016/j.jmbbm.2018.01.033.
[43] A. Gugliuzza, Solvent swollen polymer, Encycl. Membr. (2016) 1801–1802, https://doi.org/10.1007/978-3-662-44324-8_1407.
[44] E.J. Kappert, M.J.T. Raaijmakers, K. Tempelman, F.P. Cuperus, W. Ogieglo, N. E. Benes, Swelling of 9 polymers commonly employed for solvent-resistant nanofiltration membranes: a comprehensive dataset, J. Memb. Sci. 569 (2019) 177–199, https://doi.org/10.1016/j.memsci.2018.09.059.
[45] J.S. Papanu, D.W. Hess, D.S. Soane (Soong), A.T. Bell, Swelling of poly(methyl methacrylate) thin films in low molecular weight alcohols, J. Appl. Polym. Sci. 39 (1990) 803–823, https://doi.org/10.1002/APP.1990.070390404.
[46] D. Keskin, T. Mokabbar, Y. Pei, P. van Rijn, The relationship between bulk silicone and benzophenone-initiated hydrogel coating properties, Polymers (basel). 10 (2018), https://doi.org/10.3390/polym10050534.
[47] B.M. Maher, J. Rezaali, K. Jalili, F. Abbasi, Effects of various treatments on silicone rubber surface, Rubber Chem. Technol. 90 (2017) 108–125, https://doi.org/10.5254/RCT.16.83782.
[48] C.C. Shih, Y.Y. Su, L.C. Chen, C.M. Shih, S.J. Lin, Degradation of 316L stainless steel sternal wire by steam sterilization, Acta Biomater. 6 (2010) 2322–2328, https://doi.org/10.1016/J.ACTBIO.2009.12.026.
[49] A. Balamurugan, S. Rajeswari, G. Balossier, A.H.S. Rebelo, J.M.F. Ferreira, Corrosion aspects of metallic implants — an overview, Mater. Corros. 59 (2008) 855–869, https://doi.org/10.1002/MACO.200804173.
[50] T.-L. Yau, V.E. Annamalai, Corrosion of zirconium and its alloys, Ref. Modul. Mater. Sci. Mater. Eng. (2016), https://doi.org/10.1016/B978-0-12-803581-8.01641-6.
[51] A. Apratim, P. Eachempati, K.K.K. Salian, V. Singh, S. Chhabra, S. Shah, Zirconia in dental implantology: a review, J. Int. Soc. Prev. Community Dent. 5 (2015) 147, https://doi.org/10.4103/2231-0762.158014.
[52] S.M. Kurtz, J.N. Devine, PEEK biomaterials in trauma, orthopedic, and spinal implants, Biomaterials. 28 (2007) 4845–4869, https://doi.org/10.1016/j.biomaterials.2007.07.013.
[53] L. Bathala, V. Majeti, N. Rachuri, N. Singh, S. Gedela, The role of polyether ether ketone (Peek) in dentistry - a review, J. Med. Life. 12 (2019) 5–9, https://doi.org/10.25122/jml-2019-0003.
[54] I.V. Panayotov, V. Orti, F. Cuisinier, J. Yachouh, Polyetheretherketone (PEEK) for medical applications, J. Mater. Sci. Mater. Med. 27 (2016) 1–11, https://doi.org/10.1007/S10856-016-5731-4/FIGURES/3.
[55] Z. Novotna, A. Reznickova, S. Rimpelova, M. Vesely, Z. Kolska, V. Svorcik, Tailoring of PEEK bioactivity for improved cell interaction: Plasma treatment in action, RSC Adv. 5 (2015) 41428–41436, https://doi.org/10.1039/c5ra03861h.
[56] D.S. Green A, Polyaryletherketone Biomaterial for use in Medical Implant Applications 2006.
[57] T.J. Kinnari, J. Esteban, N. Zamora, R. Fernandez, C. López-Santos, F. Yubero, D. Mariscal, J.A. Puertolas, E. Gomez-Barrena, Effect of surface roughness and sterilization on bacterial adherence to ultra-high molecular weight polyethylene, Clin. Microbiol. Infect. 16 (2010) 1036–1041, https://doi.org/10.1111/J.1469-0691.2009.02995.X.
[58] M.D. Morales-Moctezuma, S.G. Spain, The effects of cononsolvents on the synthesis of responsive particles via polymerisation-induced thermal self-assembly, Polym. Chem. 12 (2021) 4696–4706, https://doi.org/10.1039/D1PY00396H.
[59] H. Kawaguchi, On going to a new era of microgel exhibiting volume phase transition, Gels (basel, Switzerland). 6 (2020) 1–24, https://doi.org/10.3390/GELS6030026.
[60] S. Backes, P. Krause, W. Tabaka, M.U. Witt, D. Mukherji, K. Kremer, R. Von Klitzing, Poly(N-isopropylacrylamide) microgels under alcoholic intoxication: when a LCST polymer shows swelling with increasing temperature, ACS Macro Lett. 6 (2017) 1042–1046, https://doi.org/10.1021/ACSMACROLETT.7B00557.
[61] Y.M. Sun, W. Wang, Y.Y. Wei, N.N. Deng, Z. Liu, X.J. Ju, R. Xie, L.Y. Chu, In situ fabrication of a temperature- and ethanol-responsive smart membrane in a microchip, Lab Chip. 14 (2014) 2418–2427, https://doi.org/10.1039/C4LC00273C.
[62] H. Senff, W. Richtering, Influence of cross-link density on rheological properties of temperature-sensitive microgel suspensions, Colloid Polym. Sci. 2789 (278) (2000) 830–840, https://doi.org/10.1007/S003960000329.
[63] M.J. Bergman, N. Gnan, M. Obiols-Rabasa, J.M. Meijer, L. Rovigatti, E. Zaccarelli, P. Schurtenberger, A new look at effective interactions between microgel particles, Nat. Commun. 9 (2018), https://doi.org/10.1038/S41467-018-07332-5.
[64] M. Vicario-De-la-torre, J. Forcada, The Potential of Stimuli-Responsive Nanogels in Drug and Active Molecule Delivery for Targeted Therapy, Gels 2017, Vol. 3, Page 16. 3 (2017) 16. https://doi.org/10.3390/GELS3020016.